Signaling across the synapse: a role for Wnt and Dishevelled in presynaptic assembly and neurotransmitter release

Azlina Ahmad-Annuar,[1] Lorenza Ciani,[1] Iordanis Simeonidis,[1] Judit Herreros,[1] Naila Ben Fredj,[1] Silvana B. Rosso,[1] Anita Hall,[1] Stephen Brickley,[2] and Patricia C. Salinas[1]

[1]Department of Anatomy and Developmental Biology, University College London, London WC1E 6BT, England, UK
[2]Department of Biological Sciences, Imperial College London, London SW8 2AY, England, UK

Proper dialogue between presynaptic neurons and their targets is essential for correct synaptic assembly and function. At central synapses, Wnt proteins function as retrograde signals to regulate axon remodeling and the accumulation of presynaptic proteins. Loss of *Wnt7a* function leads to defects in the localization of presynaptic markers and in the morphology of the presynaptic axons. We show that loss of function of Dishevelled-1 (Dvl1) mimics and enhances the *Wnt7a* phenotype in the cerebellum. Although active zones appear normal, electrophysiological recordings in cerebellar slices from *Wnt7a/Dvl1* double mutant mice reveal a defect in neurotransmitter release at mossy fiber–granule cell synapses. Deficiency in *Dvl1* decreases, whereas exposure to Wnt increases, synaptic vesicle recycling in mossy fibers. Dvl increases the number of Bassoon clusters, and like other components of the Wnt pathway, it localizes to synaptic sites. These findings demonstrate that Wnts signal across the synapse on Dvl-expressing presynaptic terminals to regulate synaptic assembly and suggest a potential novel function for Wnts in neurotransmitter release.

Introduction

During the formation of synaptic connections, axons remodel and begin to assemble the machinery required for neurotransmitter release upon arrival to their synaptic targets. An intrinsic genetic program is likely to regulate the synthesis of synaptic components and their targeting to pre- and postsynaptic sites. It is becoming clear that the cross communication between the pre- and postsynaptic terminals is essential for the coordinated assembly at both sides of the synapse. Although great emphasis has been given to the role of membrane-bound proteins such as neuroligin–neurexin (Scheiffele et al., 2000) and cadherins in this process, there is increasing evidence that secreted molecules such as Wnt, fibroblast growth factor (FGF), and TGFβ also play a crucial role in synaptic assembly and growth (Hall et al., 2000; Withers et al., 2000; Packard et al., 2002; McCabe et al., 2003; Umemori et al., 2004). However, little is known about the mechanisms by which these signals regulate synapse formation and to what extent changes in synaptic assembly translate into function.

Recent studies on neuroligin and neurexin have strengthened their role in synapse formation, as these molecules provide a local signal that stimulates synaptic assembly. Consistent with this notion, neuroligin and neurexin interact with components of the synaptic machinery (for review see Dean and Dresbach, 2006). In contrast, a distinct role for Wnts, FGFs, and thrombospondin has been proposed (Waites et al., 2005). In this model, these secreted signals could indirectly regulate synaptic formation by accelerating neuronal maturation through changes in the transcription and/or translation of synaptic components (Waites et al., 2005). Thus, synapses are formed through a sequence of events in which secreted factors stimulate neuronal maturation, thus, priming neurons for synapse formation followed by the focal action of membrane proteins that stimulate synaptic assembly. However, this model has not been fully tested and,

A. Ahmad-Annuar, L. Ciani, I. Simeonidis, and J. Herreros contributed equally to this paper.

Correspondence to Patricia C. Salinas: p.salinas@ucl.ac.uk

J. Herreros's present address is Hospital Universitari Arnau de Vilanova, Universitat de Lleida, 25198 Lleida, Spain.

A. Hall's present address is Dept. of Biological Sciences, Imperial College London, London SW8 2AY, UK.

Abbreviations used in this paper: ANOVA, analysis of variance; CASK, calmodulin-associated serine/threonine kinase; CM, conditioned media; DIV, days in vitro; FGF, fibroblast growth factor; GC, granule cell; mEPFC, miniature excitatory postsynaptic current; MF, mossy fiber; P, postnatal day.

The online version of this article contains supplemental material.

The Journal of Cell Biology, Vol. 174, No. 1, July 3, 2006 127–139
http://www.jcb.org/cgi/doi/10.1083/jcb.200511054

hence, the precise role for secreted molecules in synapse formation remains to be established.

Wnt signaling plays a key role in diverse aspects of neuronal connectivity by regulating axon guidance, dendritic development, axon remodeling and synapse formation (Ciani and Salinas, 2005). In the cerebellum, *Wnt7a* is expressed in granule cells (GCs) at the time when mossy fiber (MF) axons, their presynaptic partners, reach the cerebellar cortex and make synaptic contact with GCs (Lucas and Salinas, 1997). Upon contact, MF terminals are extensively remodeled, resulting in the formation of complex and elaborate structures called glomerular rosettes (Hamori and Somogyi, 1983a). The extensive interdigitation of several GC dendrites into a single MF axon leads to a significant increase in the area of contact and is thought to contribute to some of the unusual functional properties observed at the MF-GC synapse (DiGregorio et al., 2002; Xu-Friedman and Regehr, 2003). These morphological changes are concurrent with the accumulation of presynaptic proteins and the formation of active zones. In *Wnt7a*-deficient mice, this extensive remodeling is affected, and the accumulation of the presynaptic protein synapsin I at glomerular rosettes is delayed (Hall et al., 2000). Conversely, gain of function of Wnt7a increases the remodeling and clustering of synapsin I in MF axons in vitro (Hall et al., 2000). Thus, Wnt7a functions as a retrograde GC signal that acts on MF axons to regulate presynaptic differentiation.

The signaling pathway activated by Wnt7a during synaptogenesis remains unknown. During early development, Wnt proteins signal through at least three pathways (Fig. 1 A). Signaling through Frizzled and, in some instances through Ryk, has been shown to require the cytoplasmic scaffold protein Dishevelled (Dvl; Cadigan and Liu, 2006). However, the discovery of new Wnt receptors (Mikels and Nusse, 2006) raises the question of whether Dvl is an absolute requirement for all Wnt-mediated functions. In the β-catenin pathway, Wnts activate Dvl to inhibit the serine/threonine kinase Gsk-3β, resulting in the elevation of β-catenin levels and its subsequent translocation to the nucleus to regulate transcription (Ciani and Salinas, 2005). In neurons, lithium, which is an inhibitor of GSK-3β, mimics the remodeling and presynaptic differentiation effects of Wnt7a suggesting that the canonical pathway might be involved (Hall et al., 2000). However, the poor specificity of lithium as a Gsk-3β inhibitor poses the question as to whether Wnt7a signals through this pathway to regulate synapse formation. Thus, the downstream events leading to synapse formation induced by Wnts remain poorly understood.

To address the mechanism by which Wnt7a regulates presynaptic differentiation and to determine the functional impact of deficit in Wnt signaling, we have examined the contribution of Dvl (Logan and Nusse, 2004). New studies have revealed that Dvl functions locally within a cellular compartment (Ciani et al., 2003; Itoh et al., 2005) and can bind to microtubules to increase their stability in both dividing cells and differentiated neurons (Krylova et al., 2000). In addition, Dvl has been shown to regulate dendritic morphology in hippocampal neurons (Rosso et al., 2005). Loss of function of *Dvl1*, which is one of the three mouse *Dvl* genes, results in abnormal behavior that is manifested by defects in social interactions (Lijam et al., 1997). However, the mechanism leading to this defect remains unexplored. Interestingly, although Dvl has been shown to be involved in synapse formation at the neuromuscular junction (Luo, 2002), the role for Dvl1 at central synapses is unknown.

We examined $Dvl1^{-/-}$ mutant mice for possible defects in synapse formation and for the contribution of Dvl1 to Wnt7a function in this process. We found a functional interaction between Wnt7a and Dvl1 during the formation of the MF-GC synapse. In vivo, double $Wnt7a^{-/-}$; $Dvl1^{-/-}$ mutant mice exhibit an enhanced defect in the localization of presynaptic proteins at MF terminals when compared with single mutant mice. Ultrastructural studies reveal that glomerular rosettes in the *Wnt7a/Dvl1* mutant are simpler, yet synapses still form with normal active zones. Importantly, electrophysiological recordings of double mutant mice reveal a decreased frequency of mEPSCs without changes in amplitude, indicating a defect in neurotransmitter release. Furthermore, we show by gain and loss-of-function studies that Dvl is necessary to regulate the formation of presynaptic clusters and synaptic vesicle recycling sites. Moreover, the presence of Dvl protein at presynaptic sites and its ability to increase the clustering of Bassoon, which is a cytomatrix protein involved in synaptic assembly, are consistent with the notion that Wnt regulates synaptic assembly through Dvl. Our studies also raise the interesting possibility of a role for Wnt signaling in synaptic function.

Results

Dvl localizes to synapses

To begin to dissect the mechanism by which Wnts regulate synapse formation, we first examined the distribution of Dvl in neurons and found that endogenous Dvl is present in synaptosomal fractions isolated from adult brains (Fig. 1 B). Interestingly, other components of the Wnt pathway, such as β-catenin and Gsk-3β, are also present in synaptosomes. The specificity of this fraction was confirmed by the presence of synaptic proteins such as PSD95 and synaptophysin (Fig. 1 B). To further test whether Dvl is present at synaptic sites, we examined the colocalization of Dvl with presynaptic markers in cultured hippocampal neurons. When expressed in hippocampal neurons, Dvl1-HA has a punctate distribution along the axon and colocalizes with endogenous synapsin I (Fig. 1 C). Importantly, endogenous Dvl is found in bright and small puncta, as well as in larger and diffuse areas along the axon (Fig. 1 D). Some of the bright Dvl puncta colocalizes with endogenous clusters of synapsin I and Bassoon (Fig. 1 D). To examine whether Dvl localizes to stable synaptic sites, Dvl1-HA and PSD95-GFP were expressed in 14 d in vitro (DIV) cultures. Some Dvl1 clusters colocalize with synapsin I in close apposition with PSD95-GFP (Fig. S1, available at http://www.jcb.org/cgi/content/full/jcb.200511054/DC1). Collectively, these findings suggest that Dvl is present presynaptically at central synapses.

Wnt-Dvl signaling regulates the clustering of presynaptic markers

To test the function of Dvl in synapse formation, we examined the consequences of Wnt signaling on the formation of presynaptic

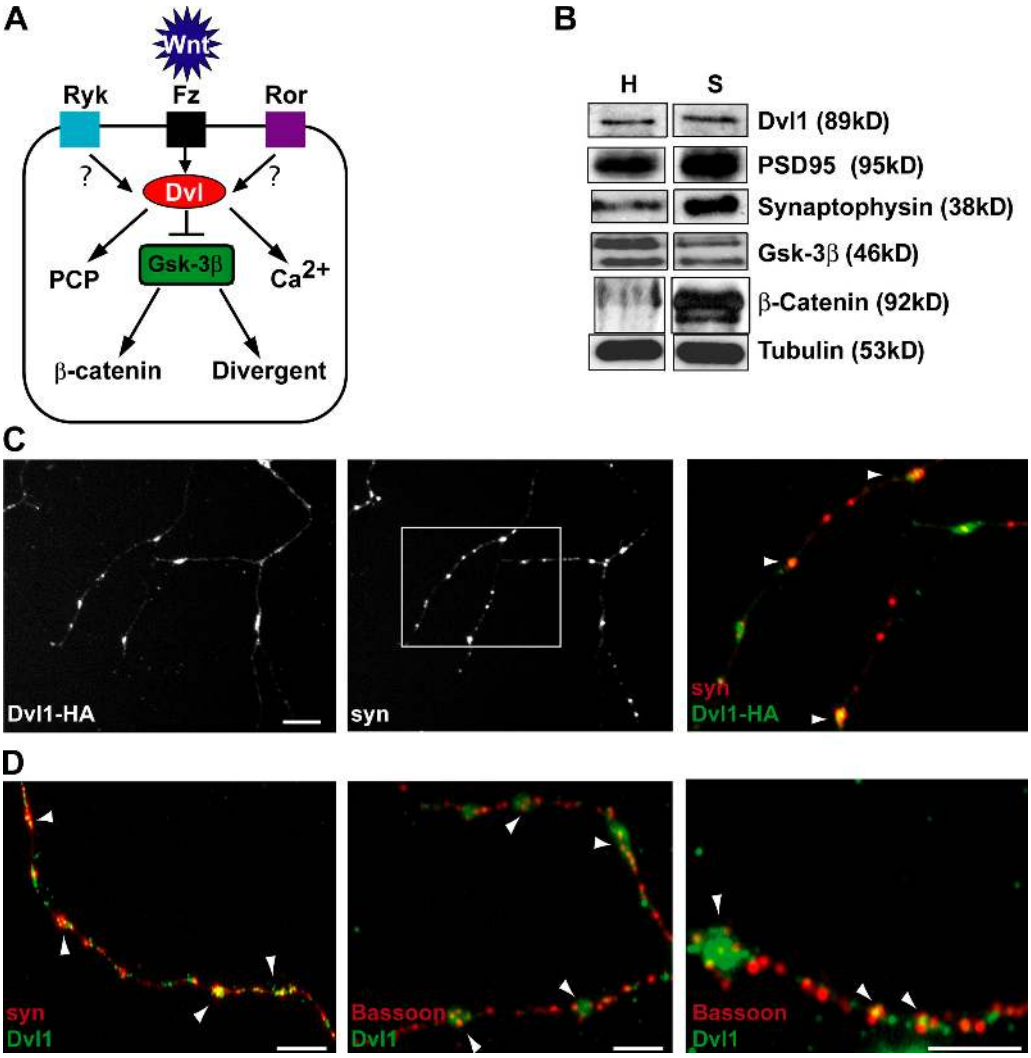

Figure 1. **Dishevelled colocalizes with presynaptic markers.** (A) Diagram illustrating the central role of Dvl in Wnt signaling pathways. PCP, planar cell polarity. Fz, Ryk, and Ror are receptors for Wnts. (B) Analyses of synaptosomes from adult mice brains show the presence of endogenous Dvl at synapses, as well as β-catenin and Gsk-3β. Synaptic proteins such as PSD95 and synaptophysin were used as specific markers for this preparation. H, total brain homogenate; S, total synaptosomal homogenate. (C) Dvl1-HA exhibits a punctate distribution along the axon of hippocampal neurons (9 DIV) as observed with endogenous synapsin I (arrowheads). Merged image shows that many of the Dvl1-HA puncta colocalize with endogenous synapsin I. (D) Staining for endogenous Dvl1 shows that Dvl colocalizes with the presynaptic marker synapsin I and the cytomatrix protein Bassoon (arrowheads). Bar, 10 μm.

clusters during the initial stages of synaptic assembly. Several studies have suggested that GC release factors, such as Wnt7a and FGF22, modulate synapse formation between MFs and GCs (Hall et al., 2000; Umemori et al., 2004). We tested the effect of GC conditioned media (CM) on the clustering of synapsin I, which provides a readout of presynaptic differentiation. We found that CM from cerebellar GCs induces the formation of numerous and very large clusters of synapsin I in MF cultures (Fig. S2 A, available at http://www.jcb.org/cgi/content/full/jcb.200511054/DC1). Wnt7a, which is released by GCs, also induces clustering, but to a lesser extent than GC-secreted factors (Fig. S2 A). Wnt7b, which is highly related to Wnt7a and is also expressed by cerebellar GCs (not shown), increases clustering of synapsin I puncta as observed with Wnt7a (Fig. S2 A). Thus, both endogenous Wnt7a and Wnt7b could regulate synapse formation between MFs and GCs in the cerebellum. The effect of Wnt7b could explain the rescue of the phenotype of the *Wnt7a* mutant at postnatal day (P) 15 (Hall et al., 2000), as expression of Wnt7b increases in GCs at this stage (unpublished data). We tested whether inhibition of Wnt activity by addition of the secreted Wnt inhibitor Sfrp-1 (Finch et al., 1997; Rattner et al., 1997) was able to block the clustering activity of GC factors. Indeed, Sfrp-1 blocks most of the clustering activity of GCs (Fig. S2 B). These findings indicate that Wnts, possibly Wnt7a and Wnt7b, contribute significantly to the clustering activity of factors released by cerebellar GCs.

To further examine the role of Wnts in presynaptic differentiation, we tested the effect of Wnts on several synaptic proteins. As Wnt7b CM exhibits a more reliable level of activity than Wnt7a CM, we have hereon used Wnt7b for gain-of-function studies. In MF axons, Wnt7b induces an 85% increase in the number of clusters labeled with VAMP2 (24 ± 2.3 clusters per 100 μm), compared with controls (13.3 ± 2.0 clusters per 100 μm; $P < 0.05$; Fig. 2, A and C). Furthermore, the Wnt antagonist Sfrp-1 blocks Wnt7b activity, as the number of VAMP2

puncta (14.1 ± 1.0 clusters per 100 μm) is similar to control (Fig. 2, A and C). In addition, VAMP2 clusters are larger in cultures exposed to Wnt7b (80.4 ± 3.3 μm^2), compared with control (51.3 ± 1.8 μm^2) and Sfrp-1 (48.2 ± 2.8 μm^2; $P < 0.05$). We then examined the effect of Wnt on the clustering of Bassoon. In 10 DIV hippocampal cultures, Wnt7b induces a 28% increase in the number of Bassoon puncta with 22.8 ± 1.9 clusters per 100 μm, compared with 17.7 ± 1.5 clusters per 100 μm in control (Fig. 2, B and D). Conversely, Sfrp1 reduces the Wnt effect to almost control levels (18.2 ± 1.9 clusters per 100 μm). Western blot analysis shows that Wnt7b does not affect the level of presynaptic proteins such as synapsin I, VAMP2, Munc18, or syntaxin in cultured MFs (Fig. 2 E). In addition, β-catenin levels are unaffected (Fig. 2 E), suggesting that Wnt

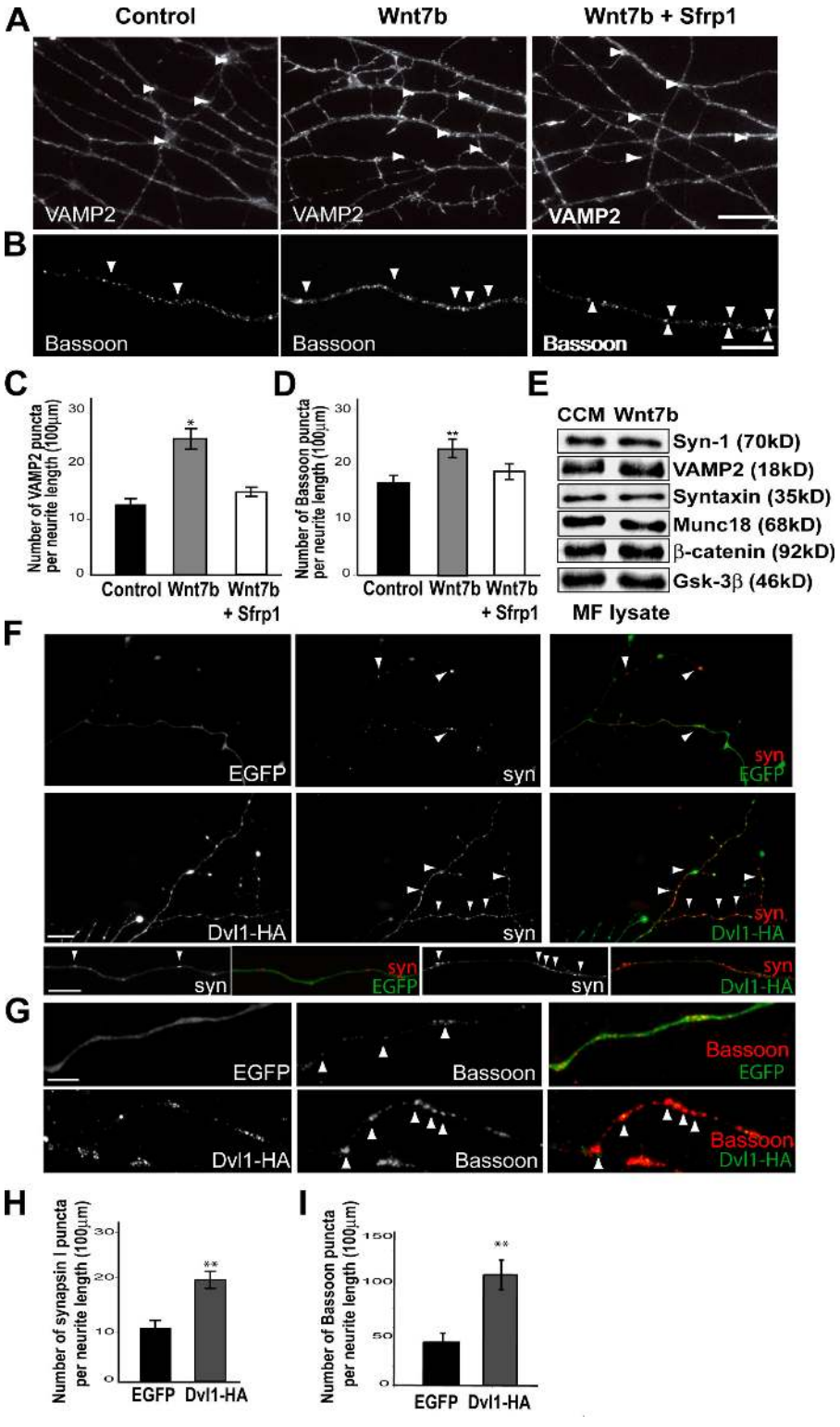

Figure 2. **Wnt signaling through Dvl1 induces synaptic vesicle clustering.** (A) MFs exposed to Wnt7b have larger and numerous VAMP2 clusters than control MFs (arrowheads). Addition of the Wnt inhibitor Sfrp-1 to Wnt7b decreases the number of VAMP2 clusters to control levels. (B) 10 DIV hippocampal neurons treated with Wnt7b have more Bassoon puncta than control or Sfrp1 cultures (arrowheads). (C and D) Quantification shows that Wnt7b induces a significant increase in the number of VAMP2 and Bassoon clusters per 100-μm axon length, and that Sfrp-1 blocks this effect to almost control levels. (E) Western blots reveal that Wnt7b does not change the levels of VAMP2, synapsin I, Munc18, syntaxin, or β-catenin proteins in MFs compared with control CM (CCM). (F) Hippocampal neurons were transfected with Dvl1-HA or EGFP before plating and cultured for 9 DIV. Neurons expressing control EGFP exhibit few and faint synapsin I clusters. In contrast, neurons expressing Dvl1-HA have larger and more numerous synapsin I clusters compared with control EGFP (arrowheads). Images at high magnification (bottom) show more synapsin I puncta (arrowheads) in Dvl-HA–expressing neurons than in control EGFP-transfected neurons. (G) Neuron expressing Dvl-HA contains more and larger Bassoon clusters when compared with control EGFP-expressing neurons. (H–I) Quantification shows that Dvl induces a significant increase in the number of synapsin I and Bassoon clusters. Error bars show the SEM. Bars: (A and F) 5 μm; (B) 4 μm; (E) 10 μm; (G) 3 μm.

might signal through a β-catenin–independent pathway. Alternatively, Wnt could induce small changes in β-catenin levels, which are not detectable after overnight treatment. Collectively, these findings suggest that Wnt increases the clustering of presynaptic markers without affecting the overall levels of presynaptic proteins.

To begin to address the mechanism by which Wnts regulate synaptogenesis, we examined the time course of Wnt action. We found that Wnt7b could induce clustering of VAMP2 within 15 min in MFs and hippocampal neurons without a visible effect on axon remodeling (Fig. S3, A–D, available at http://www.jcb.org/cgi/content/full/jcb.200511054/DC1). We then examined whether Dvl mimics the effect of Wnts on synaptic protein clustering. As explants of MFs cannot be easily transfected, we used hippocampal cultures. In EGFP-expressing control neurons, few synapsin I clusters are found along the axon (Fig. 2 F), which is similar to untransfected cells in these early cultures. In contrast, Dvl1-HA–expressing neurons exhibit a twofold increase in the number of synapsin I clusters (Fig. 2, F and H). Importantly, expression of Dvl also increases the number of Bassoon clusters by 50% (Fig. 2, G and I). Thus, Dvl1 mimics the effect of Wnts on the clustering of presynaptic markers, which is a readout of presynaptic differentiation.

We then examined the consequence of *Dvl1* loss of function. MFs isolated from wild-type mice contain 28.3 ± 1.6 clusters of VAMP2 per 100 μm (Fig. 3, A and B). In contrast, MFs from *Dvl1* mutant mice exhibit a 57% decrease in the number of VAMP2 puncta (16.0 ± 1.2 clusters per 100 μm; $P < 0.05$; Fig. 3, A and B). Furthermore, the average size of VAMP2 clusters in wild-type MFs is 53.9 ± 3.5 μm^2, whereas MFs from *Dvl1* mutant have an average size of 37.3 ± 2.6 μm^2, demonstrating that the loss of *Dvl1* function leads to a 44% decrease in the size of VAMP2 clusters ($P < 0.01$). Loss of function of both *Wnt7a* and *Dvl1* in presynaptic differentiation also results in a significant decrease in the number of VAMP2 clusters to similar levels to *Dvl1* mutant MFs (Fig. S3, E and F). This finding is consistent with the fact that isolated MFs from pontine nuclei have not yet been exposed to endogenous Wnt7a from GCs, as they were isolated before contacting GCs in the cerebellum. Interestingly, some presynaptic differentiation still occurs in *Dvl1* mutant MFs. The expression of *Dvl2* and *Dvl3* in MFs (unpublished data) could contribute to the residual level of presynaptic differentiation in the *Dvl1* mutant. Consistent with this view, we found that exposure of *Dvl1* mutant MFs to Wnt7b does result in a small increase in the number of VAMP2 clusters, but does not fully rescue the *Dvl1* phenotype to wild-type levels (Fig. 3, C and D). Collectively, these results demonstrate that *Dvl1* is required for optimal Wnt signaling to mediate presynaptic differentiation.

Wnt and Dvl1 regulate synaptic vesicle recycling

The aforementioned results suggest that Wnt signaling through Dvl1 regulates presynaptic differentiation by increasing the assembly of presynaptic sites. To test this directly, we have examined the effect of Wnt7b on synaptic vesicle recycling in MFs. Synaptic vesicle recycling was determined by the uptake of an antibody against the intralumenal domain of synaptotagmin (Matteoli et al., 1992; Kraszewski et al., 1995). Upon depolarization with a high potassium buffer, the synaptotagmin antibody is detected in vesicles corresponding to the readily releasable and reserve pools of synaptic vesicles, which have undergone exocytosis and endocytosis (Sudhof et al., 1993; Kraszewski et al., 1995). Consistent with a role in presynaptic assembly, Wnt7b increases the number of recycling puncta labeled by anti-synaptotagmin antibody by ∼61% (31.4 ± 2.2 puncta

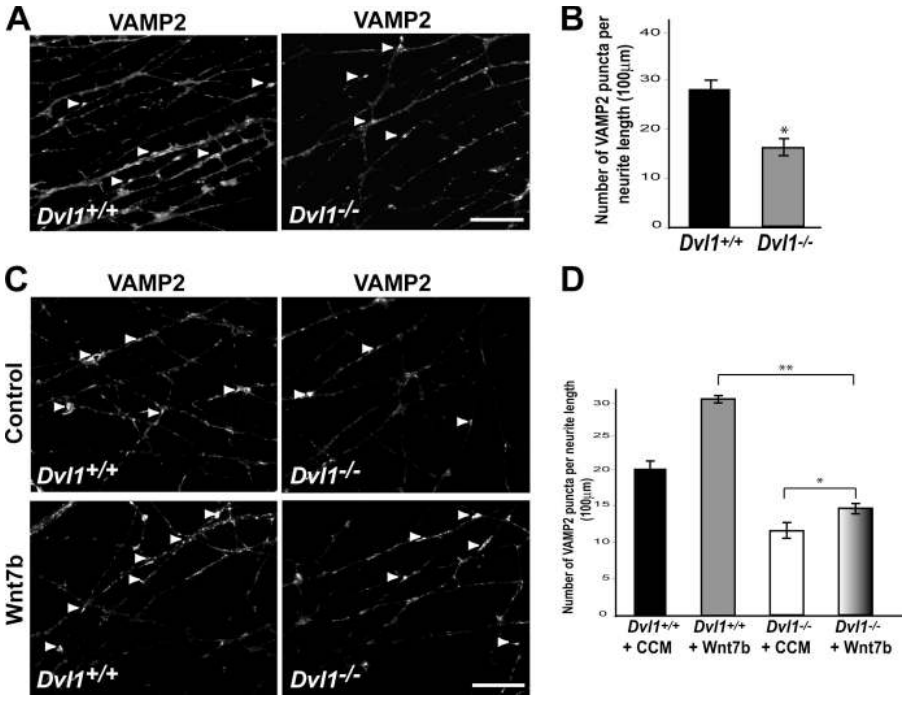

Figure 3. **Dvl1 is required presynaptically to mediate Wnt7b signaling.** (A) MFs from *Dvl1* mutant mice have fewer and smaller VAMP2 clusters than MFs from wild-type mice after 72 h in culture (arrowheads). (B) Quantification shows that *Dvl1* mutant MFs exhibit a statistically significant decrease in the number of VAMP2 clusters compared with wild-type MFs (arrowheads). (C) Wild-type and *Dvl1* mutant MFs were treated with control CM (CCM) and Wnt7b CM for 16 h. Wnt7b only partially rescues the number of VAMP2 puncta in *Dvl1* mutant MFs. (D) Quantification shows that Wnt7b induces a 40% increase in the number of VAMP2 puncta in wild-type MFs, but only a 20% increase in *Dvl1* mutant MFs. Graphs show the number of synaptic vesicle puncta per 100 μm neurite length ± the SEM. Error bars show the SEM. Asterisks indicate *, $P < 0.05$; **, $P < 0.01$. Bars, 5 μm.

per 100 μm) when compared with controls (18.9 ± 2.8 puncta per 100 μm; $P < 0.01$; Fig. 4, A and B). Importantly, the presence of Sfrp-1 significantly reduces the number of recycling vesicles when compared with Wnt7b CM (16.7 ± 3.1 puncta per 100 μm; Fig. 4, A and B). Wnt7b also induces a significant increase (57%) in the size of recycling clusters (85.4 ± 4.7 μm^2) compared with control (49.1 ± 3.5 μm^2) or Sfrp-1–treated cultures (53.2 ± 2.8 μm^2; $P < 0.05$). Western blot analyses showed that Wnt7b does not affect the level of synaptotagmin protein (Fig. 4 E), indicating that the increased number of recycling puncta reflects a true increase in the recycling rate. Moreover, synaptic vesicle recycling measured by FM1-43 dye uptake also showed that Wnt7b increases recycling (Fig. 4, C and D). These results demonstrate that Wnt7b regulates the formation of functional presynaptic terminals.

To test the requirement of Dvl1 in synaptic vesicle recycling, MFs from *Dvl1* mutant mice were examined. We used pontine explants from P0 animals when MFs have not yet been in contact with *Wnt7a*-expressing GCs. MFs from *Dvl1* mutant mice exhibit a 37% decrease in the number of recycling puncta (25 ± 1.4 puncta per 100 μm) compared with wild type (34 ± 2.0 puncta per 100 μm; $P < 0.05$; Fig. 4, F and G). The recycling clusters are also significantly smaller in *Dvl1* mutant MFs (22.9 ± 1.6 μm^2) compared with wild type (30.8 ± 2.2 μm^2; $P < 0.05$). These results indicate that *Dvl1* is required in MF terminals for normal synaptic vesicle recycling.

Deficiency in *Wnt7a* and *Dvl1* decreases the accumulation of several presynaptic proteins at cerebellar glomerular rosettes

Our previous study demonstrated that *Wnt7a*-null mutant mice exhibit a defect in synaptic differentiation that is manifested by a delayed accumulation of synapsin I at MF terminals between P10 and P12 (Hall et al., 2000). By P15, this defect is no longer evident (Hall et al., 2000). This could be caused by compensation by other factors, possibly by other Wnts like Wnt7b, which are expressed in the cerebellum. Therefore, we decided to examine the consequence of the loss of function of *Dvl1* during synapse formation. *Dvl1* is highly expressed in the cerebellum (Sussman et al., 1994; Krylova et al., 2000) and, thus, could

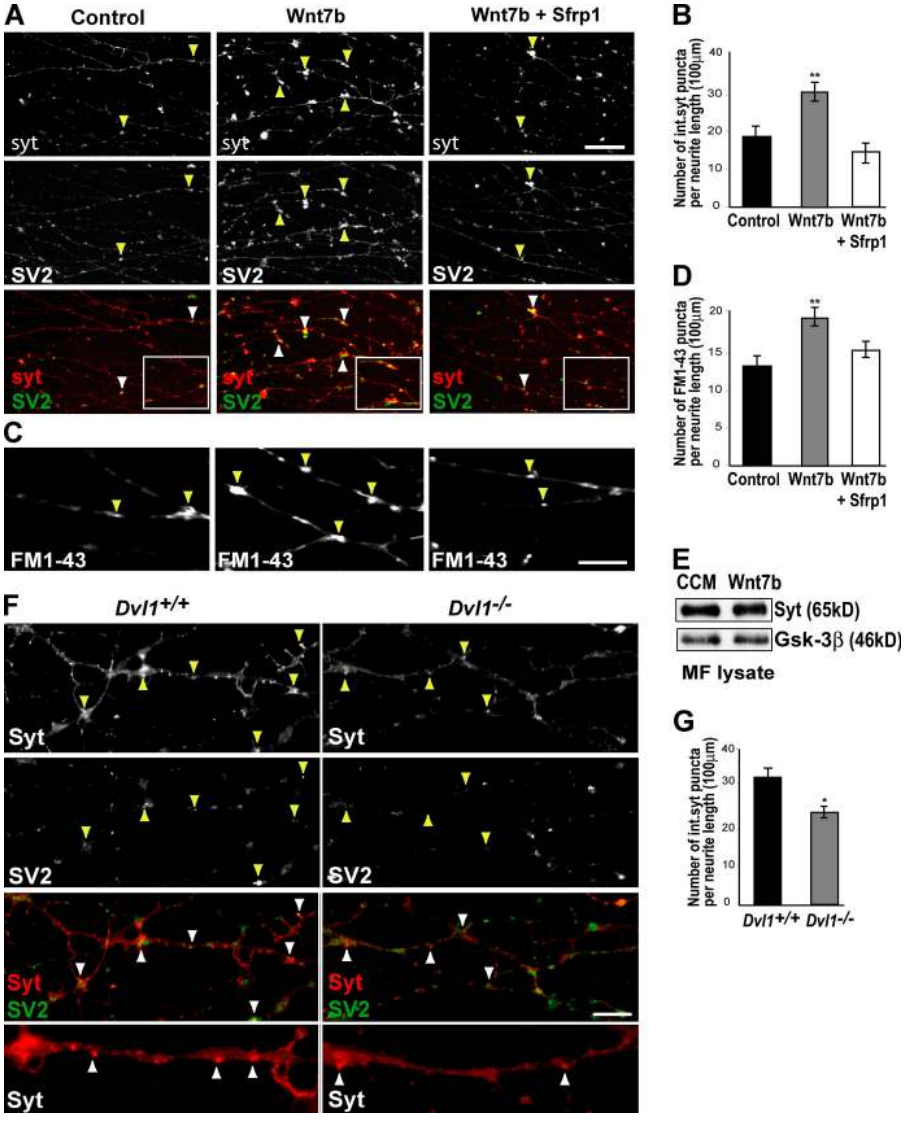

Figure 4. **Recycling activity of synaptic vesicles is mediated by Wnt signaling.** Synaptic vesicle recycling in MFs are visualized by the uptake of FM1-43 or intralumenal synaptotagmin (syt) antibody and counterstained with SV2. (A and C) Wnt7b increases the number of anti-synaptotagmin and FM1-43 recycling sites (arrowheads) compared with control MF axons, and the presence of Sfrp-1 blocks this effect. For synaptotagmin uptake, merged figures show colocalization of puncta labeled with anti-synaptotagmin with the synaptic vesicle protein SV2 (arrowheads). (B and D) Quantification shows that Wnt7b increases the number of recycling sites of anti-synaptotagmin antibody and FM1-43 uptake per 100-μm neurite length whereas Sfrp-1 blocks the activity of Wnt7b. (E) Western blot reveals that Wnt7b does not affect the level of synaptotagmin protein in MFs compared with control CM (CCM). (F) *Dvl1*$^{-/-}$ mutant MFs have fewer synaptic vesicle recycling sites when compared with wild-type MFs (arrowheads). (G) Quantification of the number of recycling sites per 100-μm neurite length indicates a 37% decrease in MFs from *Dvl1*$^{-/-}$ mutants when compared with wild-type. Error bars show the SEM. *, $P < 0.05$; **, $P < 0.01$. Bars: (A and C) 10 μm; (F) 5 μm.

mediate Wnt7a function. Importantly, MFs from *Dvl1* mutants exhibit a defect in presynaptic differentiation. To test a possible genetic interaction between *Wnt7a* and *Dvl1 in vivo*, we also examined the cerebellum of double mutant mice. Interestingly, genetic studies in *Drosophila melanogaster* have shown that defects in hypomorphic wingless/Wnt mutants can be enhanced by mutations in *dishevelled* (Theisen et al., 1994). Therefore, we predict that a concomitant loss of *Dvl1* and *Wnt7a* would enhance the *Wnt7a* phenotype.

We first analyzed *Wnt7a*, *Dvl1* single mutant, and *Wnt7a/Dvl1* double mutant mice for possible defects in the accumulation of synapsin I at P10. Indeed, *Dvl1* mutants exhibit a defect in the accumulation of synapsin I at glomerular rosettes compared with wild type, as observed in the *Wnt7a* single mutant (Fig. 5 A). More importantly, double mutant mice exhibit a stronger defect than the single mutants at P10 (Fig. 5 A). Quantification of glomerular areas stained by synapsin I revealed a shift in the size distribution of synapsin I–stained rosettes in all the mutants (Fig. 5 B), which was made evident by the increase in the percentage of smaller ($<40\ \mu m^2$) with a concomitant decrease of larger ones ($>20\ \mu m^2$; $P < 0.05$ for single mutants, $P < 0.01$ for double mutants).

We then examined glomerular rosettes at P15, which is the peak of cerebellar synaptogenesis. We found that the defect in presynaptic protein accumulation recovers by P15 in the single *Wnt7a* and *Dvl1* mutants (Fig. 5 C). In contrast, double mutant mice still exhibit a significant defect in the accumulation of synapsin I at glomerular rosettes (Fig. 5 C). Quantification shows that double mutant mice exhibit an increase of ~50% in the number of smaller synapsin I–stained glomerular rosettes ($<40\ \mu m^2$) with a concomitant decrease in the number of larger ones (Fig. 5 D). Furthermore, other presynaptic proteins, such

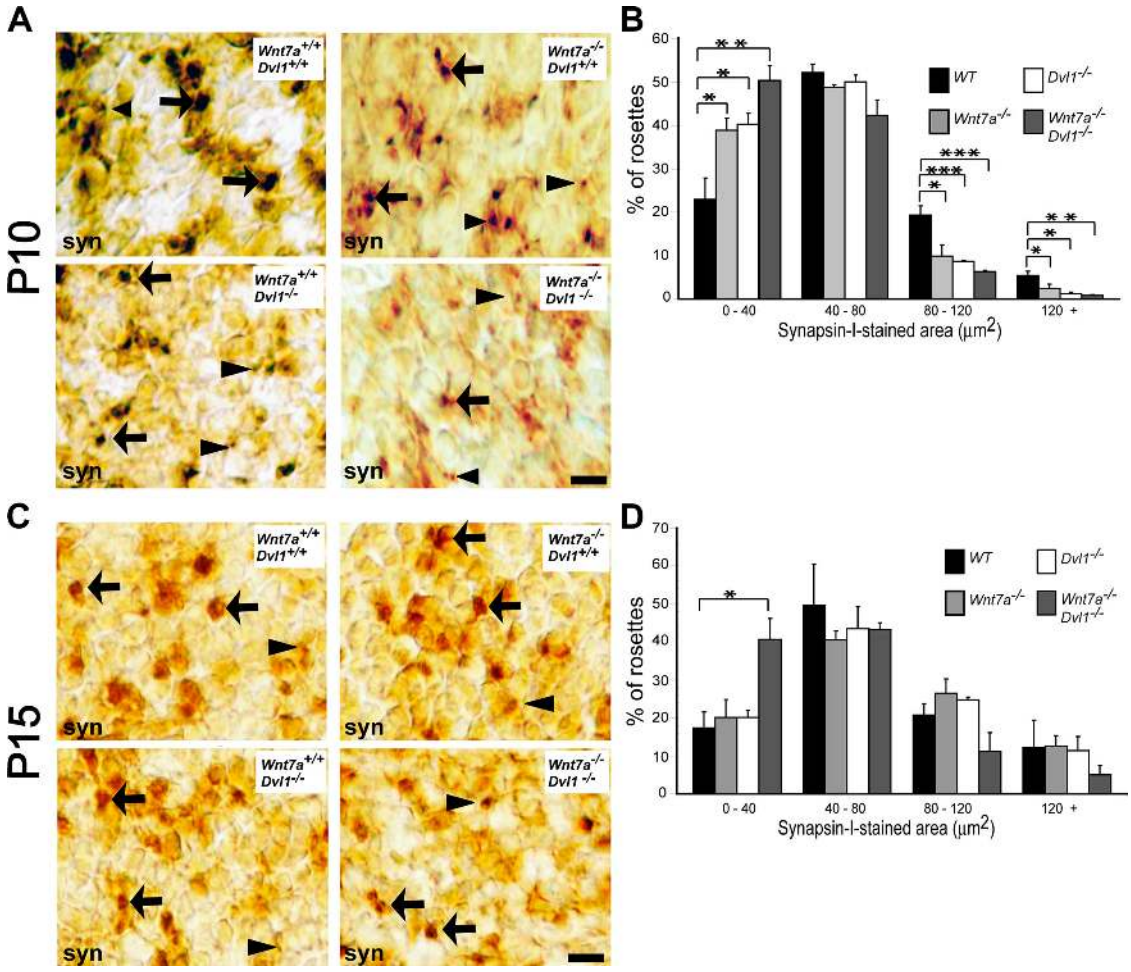

Figure 5. ***Wnt7a*$^{-/-}$*/Dvl1*$^{-/-}$ double mutant mice have smaller areas of synapsin I staining at glomerular rosettes at P10 and P15.** (A) At P10, *Wnt7a* and *Dvl1* single mutant mice exhibit a significant decrease in the number of stained glomerular rosettes when compared with wild type. This effect is significantly enhanced in *Wnt7a*$^{-/-}$; *Dvl1*$^{-/-}$ double mutant mice as the areas are less stained and smaller. (B) Size distribution of glomerular rosettes stained with synapsin I at P10 shows a significant increase in the proportion of glomerular rosettes with a size $<40\ \mu m^2$ in the double mutants (ANOVA; $P < 0.01$) when compared with wild type, and a concomitant decrease in stained rosettes with a size $>80\ \mu m^2$. Single mutants also exhibit a decrease in the smaller stained rosettes with a concomitant decrease in the large ones. (C) At P15, no significant differences are found between wild-type and single *Wnt7a* and *Dvl1* mutants. However, the double mutant still exhibits a defect. Arrows, big rosettes; arrowheads, small rosettes. (D) Size distribution of glomerular rosettes stained with synapsin I at P15 shows no differences between single mutants and wild type. However, *Wnt7a*$^{-/-}$;*Dvl1*$^{-/-}$ double mutants still exhibit a defect with a significantly larger proportion of stained rosettes with a size $<40\ \mu m^2$. Values are mean ± SEM. *, $P < 0.05$; **, $P < 0.01$; ***, $P < 0.001$. Bar, 20 μm.

as synaptobrevin/VAMP2 (Fig. S4 A, available at http://www.jcb.org/cgi/content/full/jcb.200511054/DC1), SV2 (Fig. S4 C), and synaptophysin (Fig. S4 E), were also examined at P15. Although some defects are detected in large glomerular rosettes in single mutants (Fig. S4, B, D, and F), a clear defect is observed in the double mutant, as the number of small rosettes increases with a concomitant decrease in larger rosettes (Fig. S4, B, D, and F). These findings indicate that there is a genetic interaction between *Wnt7a* and *Dvl1* at cerebellar synapses, as *Dvl1* deficiency enhances the phenotype of *Wnt7a* in cerebellar glomerular rosettes.

The defect in the localization of synaptic proteins to the presynaptic MF terminals suggests that Wnt signaling could regulate the levels of these proteins. However, Western blot analyses of whole cerebellar homogenates from P15 double mutant mice reveal no differences in the levels of VAMP2, synaptophysin, and synapsin I (Fig. S4 G). Other proteins, such as calmodulin-associated serine/threonine kinase (CASK), synaptosomal-associated protein of 25 kD, and β-catenin, are also unaffected between wild-type and double mutant mice (Fig. S4 G). These results combined with those obtained in cultured MFs indicate that Wnt7a-Dvl1 signaling regulates the distribution rather than the levels of presynaptic proteins at MF terminals during synapse formation.

Maturation of glomerular rosettes is affected in *Wnt7a/Dvl1* double mutants

During postnatal development, a single MF makes contact with several GCs to form the glomerular rosette, a multisynaptic structure. Upon contact, GCs start to interdigitate into the MF terminal, resulting in increased perimeter and complexity of this terminal (Hamori and Somogyi, 1983b). These morphological changes are correlated with synaptic maturation. Therefore, a delay in the accumulation of presynaptic proteins observed in *Wnt7a* and *Dvl1* mutants could be caused by a delay in the maturation of MFs or by a decrease in the size of the presynaptic terminal. To investigate this more closely, we analyzed the morphology of glomerular rosettes by EM at P15.

Our EM studies revealed that MF terminals have a simpler structure in the double *Wnt7a/Dvl1* mutant cerebella. We measured complexity, which was calculated based on perimeter squared divided by area (Hamori and Somogyi, 1983b), as a parameter of the irregularity of the terminal. We found that the area and complexity of MF terminals (Table I) are not significantly different between wild-type (Fig. 6, A and A'), *Wnt7a* (Fig. 6, B and B') and *Dvl1* (Fig. 6, C and C') single mutant mice (ranging from 32.30 ± 1.25 to 29.95 ± 1.09). In contrast, glomerular rosettes from double mutant mice exhibit a significant decrease in complexity (26.24 ± 0.63; $P < 0.01$; Fig. 6, D and D'). As the area of the terminals is not affected in double mutants, this finding indicates that the defect in complexity is caused by less interdigitation of GCs into the MF terminal. These results show that Wnt-Dvl signaling is required for the proper structural maturation of the MF-GC synapse in vivo. As the size of glomerular rosettes is unaffected in the mutants, the decrease in the area labeled with presynaptic proteins at glomerular rosettes (Fig. 5) is caused by a defect in the localization of presynaptic markers.

Ultrastructural analysis of *Wnt7a/Dvl1* synapse

The simpler morphology of the glomerular rosettes and the delay in the accumulation of presynaptic proteins in double mutant mice led us to examine in detail for possible structural defects at the presynaptic terminal. Several parameters were measured, including the number of synaptic contacts per glomerular rosette, the number of docked and reserve pool vesicles, the width of synaptic cleft, the length of synaptic contact, and the thickness of the postsynaptic density. Docked vesicles were defined as those vesicles present within a distance of 50 nm of the active zone, whereas the reserve pool was defined as vesicles present up to 200 nm away from the active zone (Pozzo-Miller et al., 1999). Morphometric analyses showed no significant differences in the number of synaptic contacts per glomerular rosette, in the number of docked or reserve pool vesicles between single mutant, double mutant and wild-type animals (Table I). However, double mutant mice exhibit a mild, but significant, decrease in the width of the synaptic cleft ($P < 0.01$) and the postsynaptic density ($P < 0.01$; Table I). These results suggest that apart from a defect in complexity,

Table I. **Morphometric analysis of MF–cerebellar GC synapses**

	Wild type	*Wnt7a*$^{-/-}$	*Dvl1*$^{-/-}$	*Wnt7a*$^{-/-}$, *Dvl1*$^{-/-}$
Number of synapses	6.0 ± 0.5	5.0 ± 0.5 5	5.5 ± 0.6 5.5	5.7 ± 0.6
Docked vesicles	1.9 ± 0.1	1.7 ± 0.1	1.8 ± 0.1	1.9 ± 0.1
Reserve pool vesicles	9.0 ± 0.6	9.6 ± 0.6	8.9 ± 0.7	8.4 ± 0.5
Width of synaptic cleft *(nm)*	17.6 ± 0.5	18.0 ± 0.4	18.1 ± 0.3	16.5 ± 0.4**
Width of postsynaptic density *(nm)*	20.53 ± 1.01	19.12 ± 0.82	19.59 ± 0.64	18.27 ± 0.64**
Length of synaptic contact *(μm)*	0.18 ± 0.01	0.15 ± 0.01	0.17 ± 0.01	0.17 ± 0.01
Complexity	32.3 ± 1.25	28.6 ± 1.07	29.95 ± 1.09	26.24 ± 0.63**
Perimeter *(μm)*	16.03 ± 0.68	14.76 ± 0.60	14.84 ± 0.54	13.31 ± 0.35**
Area *(μm^2)*	1.93 ± 0.12	1.81 ± 0.11	1.78 ± 0.10	1.63 ± 0.07

Morphometric analysis of MF–cerebellar GC synapses in P15 wild-type, *Wnt7a*$^{-/-}$, *Dvl1*$^{-/-}$, and *Wnt7a*$^{-/-}$;*Dvl1*$^{-/-}$ double mutant mice. The number of synapses was counted in 180 MF terminals from wild-type, *Wnt7a*$^{-/-}$, and *Dvl1*$^{-/-}$ animals ($n = 3$ per genotype) and in 300 MF terminals from *Wnt7a*$^{-/-}$;*Dvl1*$^{-/-}$ double mutant mice ($n = 5$). The n values for the quantification of the other parameters was in the range of 70–180 from three individually bred control, *Wnt7a*$^{-/-}$, and *Dvl1*$^{-/-}$ and from five *Wnt7a*$^{-/-}$;*Dvl1*$^{-/-}$ double mutant mice. Values represent the mean ± SEM. Statistical differences were assessed by ANOVA. **, $P < 0.01$.

active zones are structurally normal in single and double *Wnt7a/Dvl1* mutant mice.

Deficit in Wnt signaling affects presynaptic function

The changes in synaptic vesicle recycling in MFs observed in gain- and loss-of-function studies led us to test for possible functional defects at the MF-GC synapse. Acute cerebellar slices were used to analyze functional properties of the MF-GC synapse in the double mutant. We chose to perform electrophysiological recordings at P15, as this stage is the peak of cerebellar synaptogenesis. Importantly, P15 GCs are less heterogeneous than at earlier ages, thus, more consistent recordings can be obtained. Capacitance measurement during whole-cell voltage clamp recordings enables the measurement of estimated total membrane area (Cathala et al., 2003). We found that cerebellar GCs recorded from wild-type and double mutant mice had a similar membrane capacitance of 3.3 ± 0.3 pF ($n = 10$) and 2.9 ± 0.2 pF ($n = 10$), respectively. Thus, no significant differences in the size of cerebellar GCs between wild-type and double mutant mice were observed.

The relatively small size of cerebellar GCs means that there is little dendritic filtering of the conductance change that results from activation of postsynaptic glutamate receptors. Therefore, analysis of miniature excitatory postsynaptic currents (mEPSCs) recorded in the presence of tetrodotoxin can be used to estimate the frequency of spontaneous vesicle fusion at the MF terminal. In whole-cell recordings from wild-type GCs, mEPSCs were clearly detected in 6 out of 10 recordings, whereas in the double mutant mEPSCs were detected in 8 out of 10 recordings. The mean mEPSC frequency in wild-type GCs was 0.23 ± 0.07 Hz (Fig. 7, A, B, and G). In double mutant GCs, the mEPSC frequency was consistently lower than wild type, with an average mEPSC frequency of only 0.05 ± 0.02 Hz (Fig. 7, D, E, and G; $P < 0.05$; unpaired t test). Interestingly, single *Wnt7a* or *Dvl1* mutants showed mEPSC frequencies similar to wild type (not depicted). There were no significant differences in the mEPSC peak amplitudes (Fig. 7, C, F, and H),

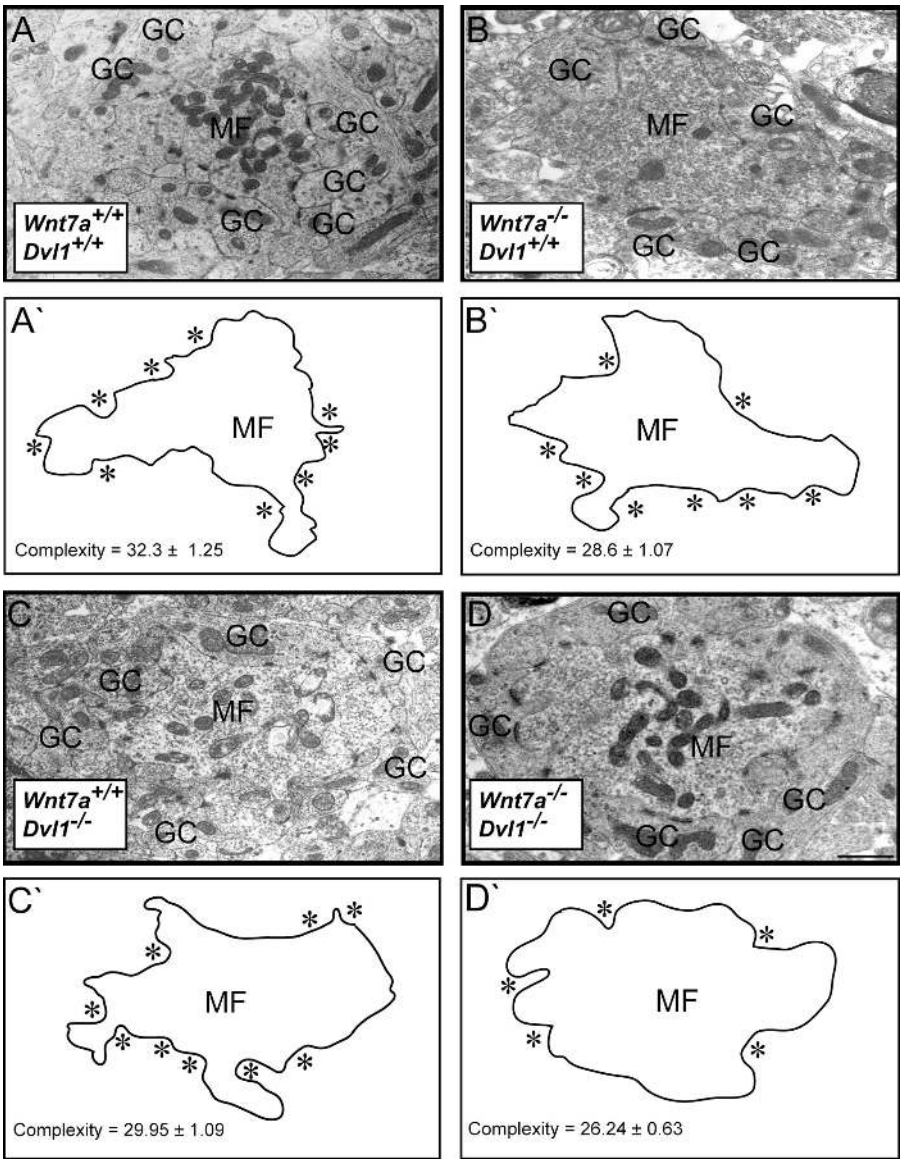

Figure 6. **Cerebellar glomerular rosettes are less complex in *Wnt7a; Dvl1* double mutants.** Electron micrographs of P15 wild-type (A), *Wnt7a* single mutant (B), *Dvl1* single mutant (C), and $Wnt7a^{-/-}/Dvl1^{-/-}$ double mutant (D) and their respective outlines (A′–D′) show the morphology of glomerular rosettes. Single mutants have complex rosettes similar to wild type (compare A, B, and C). However, the morphology of glomerular rosettes is less irregular in the $Wnt7a^{-/-}/Dvl1^{-/-}$ double mutant (D). Quantification reveals a significant decrease in the complexity (measured by perimeter^2/area) of MF terminals from double mutant animals when compared with wild-type ($P < 0.01$). In A′–D′, asterisks indicate interdigitations in the MF terminal. Values in each image represent the complexity of the terminal. Three independently bred wild-type, $Wnt7a^{-/-}$, and $Dvl1^{-/-}$ mice and five $Wnt7a^{-/-}/Dvl1^{-/-}$ double mutant animals were analyzed. 70–180 rosettes were measured per genotype. GC, GC dendrite. Bar, 0.5 μm.

10–90% rise-time, or 50% decay recorded in the either of the single knockout strains or in double mutant mice (Table S1, available at http://www.jcb.org/cgi/content/full/jcb.200511054/DC1). Therefore, a similar number of postsynaptic glutamate receptors appear to be activated after vesicle release at the MF terminal. The kinetics of activation and deactivation of these receptors were not obviously affected in any of the mutants. These results show that deficiency in *Wnt7a* or *Dvl1* alone does not affect synaptic function at this stage, but a deficiency in both *Wnt7a* and *Dvl1* results in a significant decrease of mEPSC frequency, indicating a defect in the release of neurotransmitters.

Discussion

Studies in the cerebellum and spinal cord have revealed a role for Wnt proteins as target-derived signals that regulate the terminal arborization of axons and presynaptic differentiation (Hall et al., 2000; Krylova et al., 2002). We show that Dvl1 is required for proper Wnt signaling during synapse formation. Our studies on Dvl1 have unraveled new aspects of Wnt function at central synapses. The findings presented in this study indicate that early in synaptogenesis Wnt signaling regulates the assembly of the presynaptic terminal by increasing the formation of presynaptic clusters, including Bassoon, and the number of SV recycling sites. In vivo, a deficiency of *Wnt7a* and *Dvl1* does not affect the morphology of active zones in the cerebellum, although a defect in neurotransmitter release is observed. Based on these findings, we propose a model in which Wnt signaling could regulate two processes, the assembly of the presynaptic terminal during the early stages of synaptogenesis and, later, the release of neurotransmitters.

Dvl1 is a mediator of Wnt synaptogenic activity

Dvl has been postulated to function as a scaffold protein for efficient Wnt signaling. Importantly, *Dvl1* mutant mice exhibit a defect in social behavior (Lijam et al., 1997), demonstrating that *Dvl1* deficiency affects the function of the nervous system. However, its role during synapse formation has not been explored. Our new analyses of *Dvl1* mutant mice and gain-of-function studies reveal that Dvl1 is required for the proper localization of presynaptic proteins as MF terminals from *Dvl1* mutant mice exhibit a decreased number of synaptic protein clusters and SV recycling sites. Importantly, the addition of Wnt to *Dvl1*-deficient MFs only partially restores presynaptic protein clustering. Moreover, the *Wnt7a/Dvl1* double mutant exhibits an enhanced defect in the accumulation of presynaptic proteins at cerebellar glomerular rosettes in vivo when compared

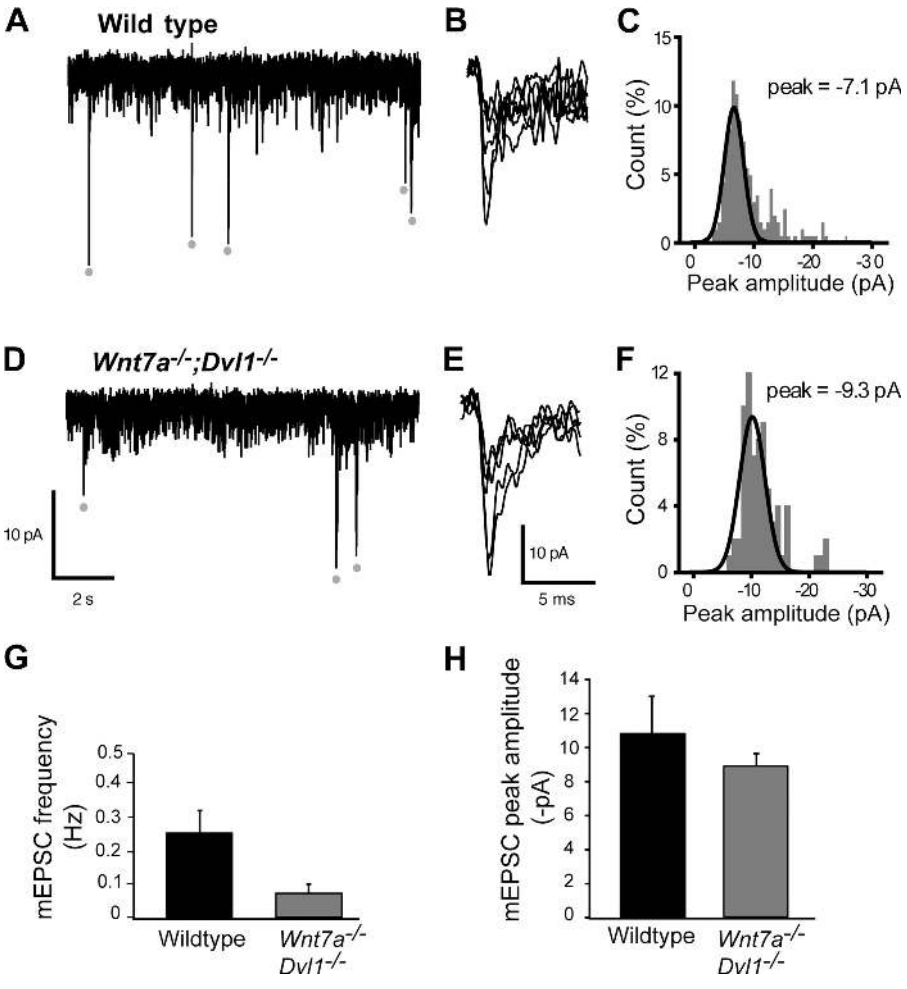

Figure 7. **The frequency of mEPSCs is reduced in *Wnt7a; Dvl1* double mutants.** Spontaneous EPSCs made from GCs of P15 mice. A representative whole-cell voltage clamp recording made from a GC in a cerebellar slice prepared from wild-type (A) and *Wnt7a*$^{-/-}$;*Dvl1*$^{-/-}$ (D) double mutant animals. In each image, detected mEPSCs (large transient inward deflections) are marked with gray circles on the continuous current record. (B and E) Superimposed spontaneous EPSCs from wild-type (B) and double mutant (E) animals. (G) Histogram shows the frequency of spontaneous EPSC from wild-type and *Wnt7a*$^{-/-}$; *Dvl1*$^{-/-}$ double mutant animals. Fewer spontaneous events occur in the *Wnt7a*$^{-/-}$; *Dvl1*$^{-/-}$ double mutant ($n = 8$) when compared with wild type ($n = 6$; unpaired *t* test). (C and F) Representative amplitude distributions from wild-type (C) and *Wnt7a*$^{-/-}$; *Dvl1*$^{-/-}$ double mutant (F) mice. (H) Histogram shows no significant differences in the amplitude of mEPSC between wild-type (-10.8 ± 2.2 pA) and *Wnt7a*$^{-/-}$; *Dvl1*$^{-/-}$ double mutant (-8.7 ± 0.9 pA) animals. Error bars indicate the SEM (unpaired *t* test).

with single *Dvl1* or *Wnt7a* mutant mice. These findings demonstrate a novel role for Dvl1 as a mediator of Wnt function during synaptogenesis in the cerebellum.

Ultrastructural analyses revealed that double mutant mice exhibit defects in the complexity of glomerular rosettes. Interestingly, the structure of the active zones is normal, with no apparent defects in the number of synaptic vesicles, despite a defect in presynaptic protein accumulation at the MF terminal. One possible interpretation for this finding is that double mutant mice might represent a partial loss of function rather than a complete loss of function of Wnt signaling. Consistent with this view, we found that *Dvl2* and *Dvl3* as well as *Wnt7b* are expressed in the cerebellum during the period of synaptogenesis (unpublished data). Thus, the presence of other *Wnts* or *Dvl* genes expressed in the cerebellum might partially compensate for the loss of *Wnt7a* and *Dvl1* function.

How does Wnt-Dvl signaling regulate synapse formation? Wnt proteins could regulate synapse formation by at least two mechanisms. Wnt could accelerate the maturation of neurons by increasing the expression of synaptic proteins and those involved in synaptic assembly. Alternatively, Wnts could regulate synaptic assembly by stimulating the localization or recruitment of synaptic components to future synaptic sites. In the first model, Wnts could regulate the transcription and/or translation of synaptic proteins. However, we found no evidence for this model, as the level of several synaptic proteins do not change in the double mutant cerebellum or in neurons exposed to Wnt. Interestingly, other secreted factors implicated in synapse formation, such as FGF22 and thrombospondin also regulate clustering without affecting the levels of presynaptic proteins (Umemori et al., 2004; Christopherson et al., 2005). In addition, we show that Dvl colocalizes with endogenous Bassoon and increases the clustering of Bassoon, which is a protein implicated in synaptic assembly. We therefore favor the view that Wnts are not just priming factors as proposed by Waites et al. (2005), but that Wnt-Dvl signaling regulates synapse formation by accelerating presynaptic assembly.

Wnts regulate presynaptic remodeling (Hall et al., 2000; Krylova et al., 2002) suggesting the possibility that Wnt-mediated effect on presynaptic differentiation could be a consequence of changes in axon morphology. However, short-term exposure of MFs to Wnt still induces presynaptic protein clustering without affecting branching and detectable changes in axon remodeling (Fig. S3, A–D). Moreover, our studies in hippocampal neurons demonstrate that Wnt7b does not induce any detectable changes in axon morphology, yet presynaptic differentiation is induced. These findings suggest that Wnt signaling regulates presynaptic assembly independently of significant changes in morphology.

Does Wnt-Dvl signaling play a role at the postsynaptic terminal? Although our studies have been focused on the presynaptic terminal, Dvl1 is also present in developing dendrites and regulates dendritic morphogenesis in hippocampal neurons (Rosso et al., 2005). Interestingly, we found a decrease in the width of the PSD at the cerebellar synapse in double mutant mice. However, no obvious changes in the amplitude of mEPSCs were observed in double mutant mice, suggesting that a similar number of postsynaptic glutamate receptors were activated after neurotransmitter release. However, further studies are needed to establish whether Wnt signaling plays a postsynaptic role.

Dvl protein is present at the synapse

Dvl was originally identified as a cytoplasmic protein that mediates Wnt signaling to the nucleus (Noordermeer et al., 1994; Siegfried et al., 1994). Recently Dvl has been shown to locally regulate signaling events within different cellular compartments (Ciani et al., 2003; Itoh et al., 2005). In neurons, we found that Dvl1 exhibits a punctate distribution along the axon as observed with many presynaptic proteins and, indeed, a pool of Dvl1 colocalizes with synapsin I and Bassoon clusters. Importantly, a fraction of Dvl clusters are in close apposition with the postsynaptic protein PSD95, suggesting that Dvl is present at both orphan and synaptic sites. Consistent with its synaptic localization in cultured neurons, endogenous Dvl1 is found in synaptosomal fractions from adult brain. These findings suggest that Wnt signaling could signal locally by activating synaptic Dvl.

Wnt-Dvl signaling regulates neurotransmitter release

Although active zones appear normal in the *Wnt7a/Dvl1* double mutant, electrophysiological recordings at the MF-GC synapse revealed a functional defect. Double mutant mice exhibit a significant decrease in the frequency of mEPSCs without affecting the amplitude and duration of mEPSCs suggesting that Wnt-Dvl signaling regulates the rate of neurotransmitter release without affecting the postsynaptic terminal.

Our studies are consistent with the notion that Wnt-Dvl signaling regulates synaptic assembly and function. Although the decrease in neurotransmitter release in the double mutant could be a consequence of an early defect in synapse formation, the fact that active zones are normal suggests that another mechanism could be involved. We propose that a partial loss of Wnt signaling permits the formation of structurally normal active zones but compromises the release of neurotransmitter by a yet unknown mechanism. Therefore, Wnt signaling could play a role in the modulation of synaptic activity in addition to synaptogenesis. Future studies will reveal whether the coordinated action of target-released molecules and membrane-bound proteins plays a role not only in synapse formation but also in synaptic modulation.

Materials and methods

Genotyping of mutant mice

All mutant mice were maintained on a C57BL/6 background. *Wnt7a;Dvl1* double mutant mice were obtained from crosses of heterozygous *Wnt7a* (A. McMahon, Harvard University, Cambridge, MA) and *Dvl1* mutant mice (T. Wynshaw-Boris, University of California, San Diego, La Jolla, CA). Genotypes were determined by three-primer PCR using tail DNA. For Wnt7a, the primers used were forward, 5′-TTCTCTTCGTGGTAGCTCTG-GGTG-3′, reverse, 5`-CTCCTTCCCGAAGACAGTACGCTCT-3′, and the forward Neo primer 5`-AGGCCTACCCGCTTCCATTGCTCA-3′. For Dvl1, the primers used were forward 5`-CGCCGCCGATCCCCTCTC-3′, reverse, 5`-TCT GCCCAATTCCACCTGCTTCTT-3′, and the Neo primer 5`-AGGCCT-ACCCGCTTCCATTGCTCA-3′.

Neuronal cultures and transfections

Basilar pontine nuclei from wild-type, *Dvl1* mutant, or *Wnt7a*$^{-/-}$;*Dvl1*$^{-/-}$ mutant mice were dissected from newborn or P1 pups, cut into 100-μm^2 explants, and cultured in 16-well LabTeck chamber slides, as previously described (Hall et al., 2000). Explants were cultured for 2 d and then treated either overnight or for 15 min with control, Wnt7b CM, or Wnt7b CM plus Sfrp-1. Untreated mutant MFs were fixed after 3 d. Hippocampal cultures were prepared from E18 rats as previously described (Dotti et al., 1988). For transfections, a Nucleofector Amaxa system was used according to the manufacturer's protocol (Amaxa Biosystems). In brief, 3×10^5 neurons were electroporated, plated at 2×10^4 neurons per coverslip, and allowed to grow for 9 d before fixation. Constructs for transfections were EGFP, Dvl1-HA, and PSD95-GFP.

Preparation of GC–secreted factors, Wnt CM, and purified Sfrp-1

CM from cerebellar GCs were prepared as described in the previous section and used to treat pontine explants. Control, Wnt7a-HA, and Wnt7b-HA CM were obtained from stably transfected Rat1b cells. Sfrp-1 CM in Fig. S2 was prepared from QT6 cells transiently transfected with myc-tagged Sfrp-1 construct (J. Nathans, Johns Hopkins University, Baltimore, MD) and used to block GC CM (Hall et al., 2000). Neuronal culture medium (N2/B27) was added to cell lines and conditioned overnight. The levels of Wnt7b and Sfrp-1 proteins were assessed by Western blot. For other blocking experiments, 2.5 μg/ml of purified Sfrp-1 (R&D Systems) was preincubated with Wnt7b CM for 20 min at room temperature before addition to neurons.

Intralumenal antisynaptotagmin antibody and FM1-43 uptake

The intralumenal antisynaptotagmin antibody uptake assay was performed as previously described (a gift from P. de Camilli, Yale University, New Haven, CT; Matteoli et al., 1992) on MFs at day 3. In brief, pontine explants were incubated for 5 min at 37°C with warm high potassium depolarization buffer; Krebs-Ringer solution (125 mM NaCl, 25 mM Hepes, pH 7.4, 5 mM KCl, 2 mM $CaCl_2$, 1.2 mM $MgSO_4$, 1.2 mM KH_2PO_4, and 6 mM glucose) supplemented with 110 mM KCl and 10 μM APV and CNQX and contained either 10 μg/ml of rabbit antiintralumenal synaptotagmin antibody or 10 μM of fixable FM1-43 (Invitrogen). After incubation, cultures were washed three times in warm Krebs-Ringer buffer, and then fixed and processed for immunofluorescence or directly mounted for FM1-43. Images were captured with a microscope (model BX60; Olympus) or with a motorized microscope (Carl Zeiss MicroImaging, Inc.) using a charge-coupled device camera (Orca ER; Hamamatsu). The number, size, and intensity of synaptotagmin puncta larger than 0.16 μm^2 were quantified using MetaMorph (Molecular Devices). As FM1-43 also labels nonsynaptic clusters, we used a more stringent threshold to select larger and brighter puncta, typically >0.20 μm^2. Axons were traced manually and the number of puncta per 100-μm neurite length and area (μm^2) were quantified. Each experiment was performed in triplicate.

Immunofluorescence microscopy

Hippocampal neurons and pontine explants were fixed with 4% paraformaldehyde, 4% sucrose in PBS (pontine explants have 0.5% EM grade glutaraldehyde added), and then permeabilized with 0.02% Triton X-100, followed by blocking with 5% BSA and incubation with primary antibodies for at least 1 h. When endogenous proteins were analyzed, neurons were fixed with methanol for 10 min at –20°C. Primary antibodies were against Dvl (Krylova et al., 2000), synaptobrevin/VAMP2 (Synaptic Systems), rabbit polyclonal intralumenal synaptotagmin (a gift from P. de Camilli), synapsin I (BD Biosciences), SV2 (Developmental Studies Hybridoma Bank), GAP-43 (Abcam), Bassoon (Bioquote Limited), and HA (Boehringer). The secondary antibodies Alexa Fluor 488 and 594 were obtained from Invitrogen. Each experiment was performed in triplicate and at least 15 images were taken per condition. The images were analyzed using MetaMorph. A threshold was set to capture clusters that were clearly distinguishable and did not merge with one another. The number, size, and intensity of the puncta were measured and Analysis of variance (ANOVA) statistical tests were performed.

Immunohistochemistry

Cerebella from wild-type and mutant animals were fixed in 4% PFA, embedded in paraffin, and processed as previously described (Hall et al., 2000). Antibodies against synapsin I, synaptophysin (CHEMICON International, Inc.), VAMP2, and SV2 were used. Localization of the proteins was visualized by the VECTASTAIN ABC peroxidase system (Vector Laboratories). Three independently bred animals were used for each of the four genotypes. An area of 2,700 glomerular rosettes per animal was measured. ANOVA statistical tests were performed.

Western blot analysis

SDS-PAGE and immunoblotting were performed from pontine explants or from cerebella using standard methods. Pontine samples were analyzed for cytoplasmic synaptotagmin (Synaptic Systems), VAMP2, synapsin I, Munc18, and β-catenin (BD Biosciences). Gsk-3β (BD Biosciences) was used as a loading control, whereas P15 cerebellar homogenates were analyzed for CASK (CHEMICON International, Inc.), synaptophysin (CHEMICON International, Inc.), VAMP2, synaptosomal-associated protein of 25 kD (Synaptic Systems), synapsin I, β-catenin, and tubulin (Abcam).

Synaptosome preparation

Synaptosomes were prepared as previously described (Cohen et al., 1977). In brief, adult mouse brains were homogenized in buffer A (0.32 M sucrose, 4 mM Hepes, pH 7.4, plus protease and phosphatase inhibitors) and centrifuged at 800 *g* for 10 min. All procedures were performed at 4°C. The supernatant was clarified by centrifugation at 9,000 *g* for 15 min, and the pellet containing myelin and synaptosomal and mitochondrial structures was resuspended in buffer A and layered on top of a discontinuous gradient containing 0.8/1.0/1.2 M sucrose in 4 mM Hepes, pH 7.4, plus protease inhibitors, and centrifuged at 82,500 *g* for 90 min. Synaptic membranes were taken from a 1–1.2-M interface and resuspended in buffer B (0.32 M sucrose, 4 mM Hepes, pH 7.4, and 150 mM NaCl plus inhibitors). Proteins were quantified by Lowry assay.

Electron microscopy

Small pieces from the internal granular layer of cerebellar lobes V, VI, and VIII of P15 animals were dissected and fixed in 3% EM grade glutaraldehyde in 0.1 M phosphate buffer, pH 7.3, at 4°C for at least 5 d. Samples from three wild-type, 3 *Wnt7a*$^{-/-}$, 3 *Dvl1*$^{-/-}$, and 5 *Wnt7a*$^{-/-}$; *Dvl1*$^{-/-}$ mice were analyzed. Tissues were processed at the EM Unit of King's College London. Photographs of whole glomerular rosettes were taken at 20,000×, whereas photographs of synapses were taken at 72,000×. Photographs were scanned and analyzed. Glomerular complexity was estimated using the formula perimeter^2/area (Hamori and Somogyi, 1983b). Docked vesicles were considered as vesicles present within 50 nm (one vesicle diameter) of the active zone, whereas vesicles located up to 200 nm away from the docked vesicles were considered as the reserve pool (Pozzo-Miller et al., 1999). ANOVA statistical tests were performed.

Electrophysiology

Parasagittal slices (250 μm thick) were cut from P14–P15 cerebellar vermis of mice. The slicing solution contained the following: 125 mM NaCl, 2.5 mM KCl, 1 mM $CaCl_2$, 2 mM $MgCl_2$, 26 mM $NaHCO_3$, 1.25 mM NaH_2PO_4, 25 mM glucose, 0.02–0.08 mM D-2-amino-5-phosphonopentanoic acid (D-AP5), pH 7.4, when bubbled with 95% O_2 and 5% CO_2. Patch-clamp recordings were made at room temperature (22–23°C), with an amplifier (Axopatch 700B; Axon Instruments). 50 mM picrotoxin and 1 mM strychnine was included in the recording solution to block $GABA_A$ and glycine receptors, respectively, and in the presence 0.5 mM TTX to isolate mEPSCs. Patch pipette "internal" solution contained the following: 140 mM CsCl, 4 mM NaCl, 0.5 mM $CaCl_2$, 10 mM Hepes, 5 mM EGTA, and 2 mM Mg-ATP (adjusted to pH 7.3 with CsOH). Data analysis was performed using custom written software (Istvan Mody and Thorsten Hodapp, University of California, Las Angeles, Los Angeles, CA). Spontaneous mEPSCs were filtered at 2 kHz and digitized at 10 kHz. As all data were normally distributed (Shapiro-Wilk test), statistical differences between groups were tested using the *t* test and considered significant at $P < 0.05$ (STATISTICA 5.1; StatSoft).

Online supplemental material

Fig. S1 shows that Dvl1 colocalizes with synapsin I at synaptic sites. Fig. S2 shows that Wnt7a and Wnt7b have similar effects on synaptic vesicle clustering. Fig. S3 shows that short-term exposure to Wnt7b is sufficient to induce presynaptic assembly in mossy fibers and hippocampal neurons and *Wnt7a*$^{-/-}$; *Dvl1*$^{-/-}$ double mutant (DKO) mossy fibers exhibit a defect in presynaptic clustering. Fig. S4 shows that *Wnt7a;Dvl1* double mutant exhibits a defect in the accumulation of several presynaptic proteins at cerebellar glomerular rosettes at P15. Table S1 shows the properties of spontaneous EPSCs in GCs from wild-type and *Wnt7a*$^{-/-}$; *Dvl1*$^{-/-}$ P15 animals. Online supplemental material is available at http://www.jcb.org/cgi/content/full/jcb.200511054/DC1.

We would like to thank to Drs. Any McMahon, Daniel Sussman, and Tony Wynshaw-Boris for generously providing the *Wnt-7a* and *Dvl1* mutant mice, Eckard Gunderfinger for the Bassoon-EGFP construct, and Jeremy Nathans for Sfrp-1 construct, Pietro de Camilli for antibodies, and John Pacy for EM processing. We also thank Angela Brennan for helping with EM analyses and members of our laboratory for useful discussion and comments on the manuscript.

The Wellcome Trust, the Biotechnology and Biological Sciences Research Council, and the Medical Research Council (to J. Herreros) supported this work.

We declare that there are no commercial affiliations or conflict of interests.

Submitted: 16 November 2005
Accepted: 30 May 2006

References

Cadigan, K.M., and Y.I. Liu. 2006. Wnt signaling: complexity at the surface. *J. Cell Sci.* 119:395–402.

Cathala, L., S. Brickley, S. Cull-Candy, and M. Farrant. 2003. Maturation of EPSCs and intrinsic membrane properties enhances precision at a cerebellar synapse. *J. Neurosci.* 23:6074–6085.

Christopherson, K.S., E.M. Ullian, C.C. Stokes, C.E. Mullowney, J.W. Hell, A. Agah, J. Lawler, D.F. Mosher, P. Bornstein, and B.A. Barres. 2005. Thrombospondins are astrocyte-secreted proteins that promote CNS synaptogenesis. *Cell*. 120:421–433.

Ciani, L., and P.C. Salinas. 2005. WNTs in the vertebrate nervous system: from patterning to neuronal connectivity. *Nat. Rev. Neurosci.* 6:351–362.

Ciani, L., O. Krylova, M. Smalley, T. Dale, and P.C. Salinas. 2003. A divergent canonical WNT signalling pathway regulates microtubule dynamics: Dishevelled signals locally to stabilize microtubules. *J. Cell Biol.* 164:243–253.

Cohen, R.S., F. Blomberg, K. Berzins, and P. Siekevitz. 1977. The structure of postsynaptic densities isolated from dog cerebral cortex. I. Overall morphology and protein composition. *J. Cell Biol.* 74:181–203.

Dean, C., and T. Dresbach. 2006. Neuroligins and neurexins: linking cell adhesion, synapse formation and cognitive function. *Trends Neurosci.* 29:21–29.

DiGregorio, D.A., Z. Nusser, and R.A. Silver. 2002. Spillover of glutamate onto synaptic AMPA receptors enhances fast transmission at a cerebellar synapse. *Neuron*. 35:521–533.

Dotti, C.G., C.A. Sullivan, and G.A. Banker. 1988. The establishment of polarity by hippocampal neurons in culture. *J. Neurosci.* 8:1454–1468.

Finch, P.W., X. He, M.J. Kelley, A. Uren, R.P. Schaudies, N.C. Popescu, S. Rudikoff, S.A. Aaronson, H.E. Varmus, and J.S. Rubin. 1997. Purification and molecular cloning of a secreted, Frizzled-related antagonist of Wnt action. *Proc. Natl. Acad. Sci. USA*. 94:6770–6775.

Hall, A.C., F.R. Lucas, and P.C. Salinas. 2000. Axonal remodeling and synaptic differentiation in the cerebellum is regulated by WNT-7a signaling. *Cell*. 100:525–535 (see comments).

Hamori, J., and J. Somogyi. 1983a. Differentiation of cerebellar mossy fiber synapses in the rat: a quantitative electron microscope study. *J. Comp. Neurol.* 220:365–377.

Hamori, J., and J. Somogyi. 1983b. Formation of new synaptic contacts by Purkinje axon collaterals in the granular layer of deafferented cerebellar cortex of adult rat. *Acta Biol. Hung.* 34:163–176.

Itoh, K., B.K. Brott, G.U. Bae, M.J. Ratcliffe, and S.Y. Sokol. 2005. Nuclear localization is required for Dishevelled function in Wnt/beta-catenin signaling. *J. Biol.* 4:3.

Kraszewski, K., O. Mundigl, L. Daniell, C. Verderio, M. Matteoli, and P. De Camilli. 1995. Synaptic vesicle dynamics in living cultured hippocampal neurons visualized with CY3-conjugated antibodies directed against the lumenal domain of synaptotagmin. *J. Neurosci.* 15:4328–4342.

Krylova, O., M.J. Messenger, and P.C. Salinas. 2000. Dishevelled-1 regulates microtubule stability: a new function mediated by glycogen synthase kinase-3β. *J. Cell Biol.* 151:83–94.

Krylova, O., J. Herreros, K. Cleverley, E. Ehler, J. Henriquez, S. Hughes, and P. Salinas. 2002. WNT-3, Expressed by Motoneurons, Regulates Terminal Arborization of Neurotrophin-3-Responsive Spinal Sensory Neurons. *Neuron*. 35:1043-1056.

Lijam, N., R. Paylor, M.P. McDonald, J.N. Crawley, C.X. Deng, K. Herrup, K.E. Stevens, G. Maccaferri, C.J. McBain, D.J. Sussman, and A. Wynshaw-Boris. 1997. Social interaction and sensorimotor gating abnormalities in mice lacking Dvl1. *Cell*. 90:895–905.

Logan, C.Y., and R. Nusse. 2004. The Wnt signaling pathway in development and disease. *Annu. Rev. Cell Dev. Biol.* 20:781–810.

Lucas, F.R., and P.C. Salinas. 1997. WNT-7a induces axonal remodeling and increases synapsin I levels in cerebellar neurons. *Dev. Biol.* 193:31–44.

Luo, L. 2002. Actin cytoskeleton regulation in neuronal morphogenesis and structural plasticity. *Annu. Rev. Cell Dev. Biol.* 18:601–635.

Matteoli, M., K. Takei, M.S. Perin, T.C. Sudhof, and P. De Camilli. 1992. Exo-endocytotic recycling of synaptic vesicles in developing processes of cultured hippocampal neurons. *J. Cell Biol.* 117:849–861.

McCabe, B.D., G. Marques, A.P. Haghighi, R.D. Fetter, M.L. Crotty, T.E. Haerry, C.S. Goodman, and M.B. O'Connor. 2003. The BMP homolog Gbb provides a retrograde signal that regulates synaptic growth at the *Drosophila* neuromuscular junction. *Neuron*. 39:241–254.

Mikels, A.J., and R. Nusse. 2006. Purified Wnt5a protein activates or inhibits beta-catenin-TCF signaling depending on receptor context. *PLoS Biol.* 4:e115.

Noordermeer, J., J. Klingensmith, N. Perrimon, and R. Nusse. 1994. Dishevelled and armadillo act in the wingless signalling pathway in *Drosophila*. *Nature*. 367:80–83.

Packard, M., E.S. Koo, M. Gorczyca, J. Sharpe, S. Cumberledge, and V. Budnik. 2002. The Drosophila wnt, wingless, provides an essential signal for pre- and postsynaptic differentiation. *Cell*. 111:319–330.

Pozzo-Miller, L.D., W. Gottschalk, L. Zhang, K. McDermott, J. Du, R. Gopalakrishnan, C. Oho, Z.H. Sheng, and B. Lu. 1999. Impairments in high-frequency transmission, synaptic vesicle docking, and synaptic protein distribution in the hippocampus of BDNF knockout mice. *J. Neurosci.* 19:4972–4983.

Rattner, A., J.C. Hsieh, P.M. Smallwood, D.J. Gilbert, N.G. Copeland, N.A. Jenkins, and J. Nathans. 1997. A family of secreted proteins contains homology to the cysteine-rich ligand-binding domain of frizzled receptors. *Proc. Natl. Acad. Sci. USA*. 94:2859–2863.

Rosso, S.B., D. Sussman, A. Wynshaw-Boris, and P.C. Salinas. 2005. Wnt signaling through Dishevelled, Rac and JNK regulates dendritic development. *Nat. Neurosci.* 8:34–42.

Scheiffele, P., J. Fan, J. Choih, R. Fetter, and T. Serafini. 2000. Neuroligin expressed in nonneuronal cells triggers presynaptic development in contacting axons. *Cell*. 101:657–669.

Siegfried, E., E.L. Wilder, and N. Perrimon. 1994. Components of wingless signalling in *Drosophila*. *Nature*. 367:76–79.

Sudhof, T.C., A.G. Petrenko, V.P. Whittaker, and R. Jahn. 1993. Molecular approaches to synaptic vesicle exocytosis. *Prog. Brain Res.* 98:235–240.

Sussman, D.J., J. Klingensmith, P. Salinas, P.S. Adams, R. Nusse, and N. Perrimon. 1994. Isolation and characterization of a mouse homolog of the *Drosophila* segment polarity gene dishevelled. *Dev. Biol.* 166:73–86.

Theisen, H., J. Purcell, M. Bennett, D. Kansagara, A. Syed, and J.L. Marsh. 1994. Dishevelled is required during wingless signaling to establish both cell polarity and cell identity. *Development*. 120:347–360.

Umemori, H., M.W. Linhoff, D.M. Ornitz, and J.R. Sanes. 2004. FGF22 and its close relatives are presynaptic organizing molecules in the mammalian brain. *Cell*. 118:257–270.

Waites, C.L., A.M. Craig, and C.G. Garner. 2005. Mechanisms of vertebrate synaptogenesis. *Annu. Rev. Neurosci.* 28:251–274.

Withers, G.S., D. Higgins, M. Charette, and G. Banker. 2000. Bone morphogenetic protein-7 enhances dendritic growth and receptivity to innervation in cultured hippocampal neurons. *Eur. J. Neurosci.* 12:106–116.

Xu-Friedman, M.A., and W.G. Regehr. 2003. Ultrastructural contributions to desensitization at cerebellar mossy fiber to granule cell synapses. *J. Neurosci.* 23:2182–2192.

Zhai, R.G., H. Vardinon-Friedman, C. Cases-Langhoff, B. Becker, E.D. Gundelfinger, N.E. Ziv, and C.C. Garner. 2001. Assembling the presynaptic active zone: a characterization of an active one precursor vesicle. *Neuron*. 29:131–143.